[redacted]

27-750

Sunday December 11th, 2011

Professor Rollett

Introduction

The aim of this paper is to examine modern research relating to texture and anisotropy. Originally, the scope was to mainly look at phase transformations and evolution of texture, however I have expanded the scope to look at some interesting processing techniques that aim to control texture and subsequently the properties of the material in question. I try to touch upon all classes of materials that are relevant to texture and anisotropy including metals, ceramics, shape memory alloys, and composites. A wide variety of papers were reviewed, but only a select few were used to construct this literature review, a list of which can be found in the references section.

Metals: Texture Control in Steels

This section of the report addresses cold-rolled steels, and the application of annealing for the purpose of texture control. The primary reference is the comprehensive study done by R.K. Ray, J.J. Jonas, and R.E. Hook titled "Cold rolling and annealing textures in low carbon and extra low carbon steels". This paper has proven to be a very detailed and complete study on texture control in cold rolled steels, and is a valuable starting point for anyone looking to enter this field of study.

For cold rolling and drawing of steels, the goal of texture control is to maximize the degree to which the steel can be drawn in the plane, while still preventing plastic flow in the thickness direction of the rolled material. This value can be described by the relationship,

$$r_m = \frac{r_0 + 2r_{45} + r_{90}}{4}$$

where r_0,$r_{45}$and r_{90} are the ratios of strain in the width direction to the strain in the thickness direction, measured relative to the rolling direction of the sample. While maximizing r_m is the primary goal, it is important to consider other factors. Significant differences between r_{45} and r_0 or r_{90} will result in significant ear formation, similar to the ears observed on the aluminum cans presented in class. The metric used to describe the likelihood of ear formation is described as follows.

$$\Delta r = \frac{r_0 + r_{90} - 2r_{45}}{2}$$

The findings by D. Daniel and J.J. Jonas, cited by Ray et al. are summarized in Table 1, the caption is a direct quotation.

Texture Component	r_m	Δr
{001}<110>	0.4	-0.8
{112}<110>	2.1	-2.7
{111}<110>	2.6	0
{111}<112>	2.6	0
{554}<225>	2.6	1.1
{110}<001>	5.1	8.9

Table 1: Major components observed in cold rolling and annealing textures of low C steels

In Table 1, it can be seen that while the {110}<001> component has the highest r_m value (5.1), it has by far the largest susceptibility to ear formation of any of the texture components listed, with a Δr of 8.9. Far more useful components are the {111}<110> and {111}<112> components, which still have a moderate r_m value (2.6), but have a Δr of 0.

Once the anisotropy of cold drawing properties is understood, research can be done on the control of texture in various forms of steel. For a detailed review of texture control in a variety of steels including rimmed steel, Al killed steel (regular and ELC), Ti stabilized IF steels (ordinary and ELC), Nb stabilized If steels (ordinary and ELC), and Nb+Ti stabilized (ELC), the paper by Ray et al. is an excellent compendium of information in that regard. In this review, I will summarize the effects observed, including effects from hot band rolling, cold-rolling, and annealing. It has also been found that interstitial elements, substitutional elements, and precipitates play a significant role in texture development in steels, but those factors are outside the scope of this paper.

Hot Band Rolling

In hot band rolling, the primary texture formation is through the transformation from austenite to ferrite, rather than the deformation texture. For example, the {001}<100> texture in austenite becomes the {001}<110> in ferrite, though this texture is only prevalent when no recrystallization is allowed. If recrystallization is allowed then strong brass, copper, and S components occur, along with a lesser Goss component. Alloying components can induce other preferential fibers, such as {112}<110> in Nb steels and {001}<110> in Ti steels.

Cold Rolling

Beginning with the {001}<110> component in ferrite, increasing reduction causes development of a partial <110>||RD fiber as well as a {111}||ND fiber. What begins as the strongest component, {111}<110> (60% reduction), begins to shift to the {112}<110> (80%). As mentioned before, the {112}<110> is a favorable texture for the mechanical properties of the steel. It has also been found that Nb increases the {112}<110> component, and this component is also the strongest component in interstitial free steels. Figure 1 illustrates the effect of cold rolling on the r_m value, caption quoted from paper.

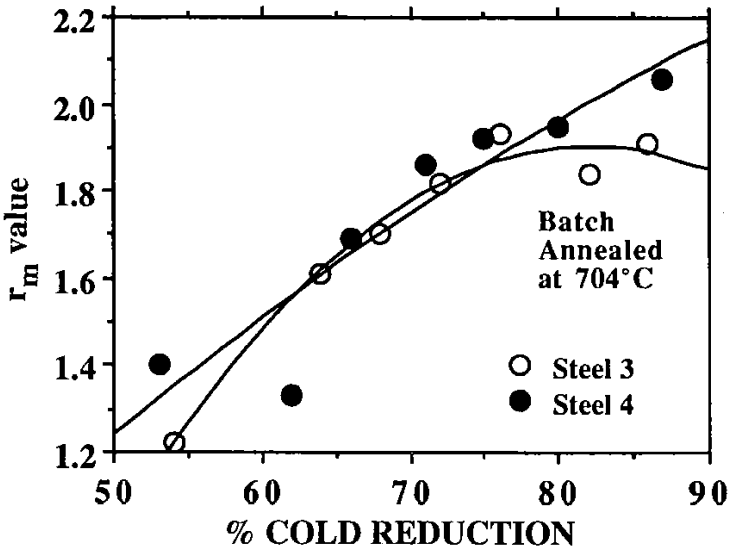

Figure 1: Effect of amount of cold reduction on r_m values of two CRBA Nb+Ti ELC IF steels

We can see that for there is a significant upward trend for r_m with increasing % Cold Reduction with fairly good correlation.

Annealing

Due to recrystallization, the partial <110>||RD fiber and the {111}||ND fiber decrease in intensity, though after time the <111> increases again. The remaining predominant component is the {111}<110> component. A variety of other factors have a strong effect on texture development, including coiling temperature, cold reduction, as well as the heating and cooling rates. Figure 2 provides a summary of the effect of heating rate on the eventual r_m value, again the caption is directly quoted from the paper.

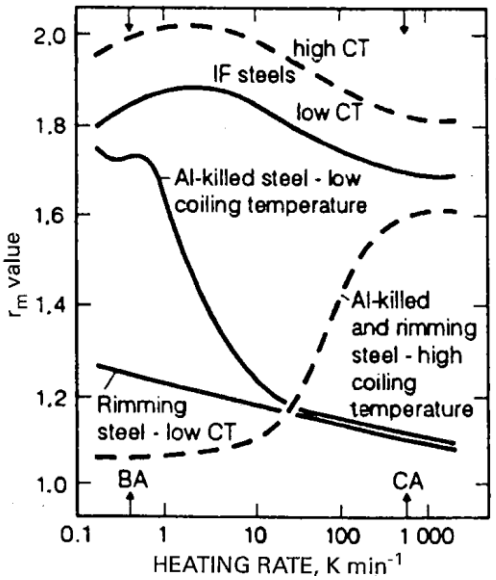

Figure 2: Effect of heating rate during annealing on r_m value of different steel types with varying coiling temperatures after hot rolling

As we can see in this figure, there are a variety of different responses to heating rate, clearly there is much more to consider in order to better perfect the material properties.

EBSD Analysis: Techniques and Applications

Since we have studied EBSD in class, I will keep this section short, focusing on a modern application studied via EBSD. The paper in review here is "Effect of cooling rate on transformation texture and variant selection during β → α transformation in Ti-5Ta-1.8Nb alloy", by T. Karthikeyan, Arup Dasgupta, R. Khatirkar, S. Saroja, I. Samajdar, and M. Vijayalakshmi. In this paper, the α→β→α transformation in the aforementioned titanium alloy is carried out through different cooling rates, and studied using EBSD and XRD techniques. The resulting microstructure from this transformation is a lamellar structure. Of particular interest is the transformation texture that the α phase derives from the original high temperature β phase. As we know, the β phase is a bcc phase, while α is an hcp phase. Use of EBSD analysis allowed researchers to carefully examine the thin β lamellae in the microstructure, which as you can see in the following figure (captions from text), were much smaller than the α regions (indicated by green), the β regions are primarily (111) texture.

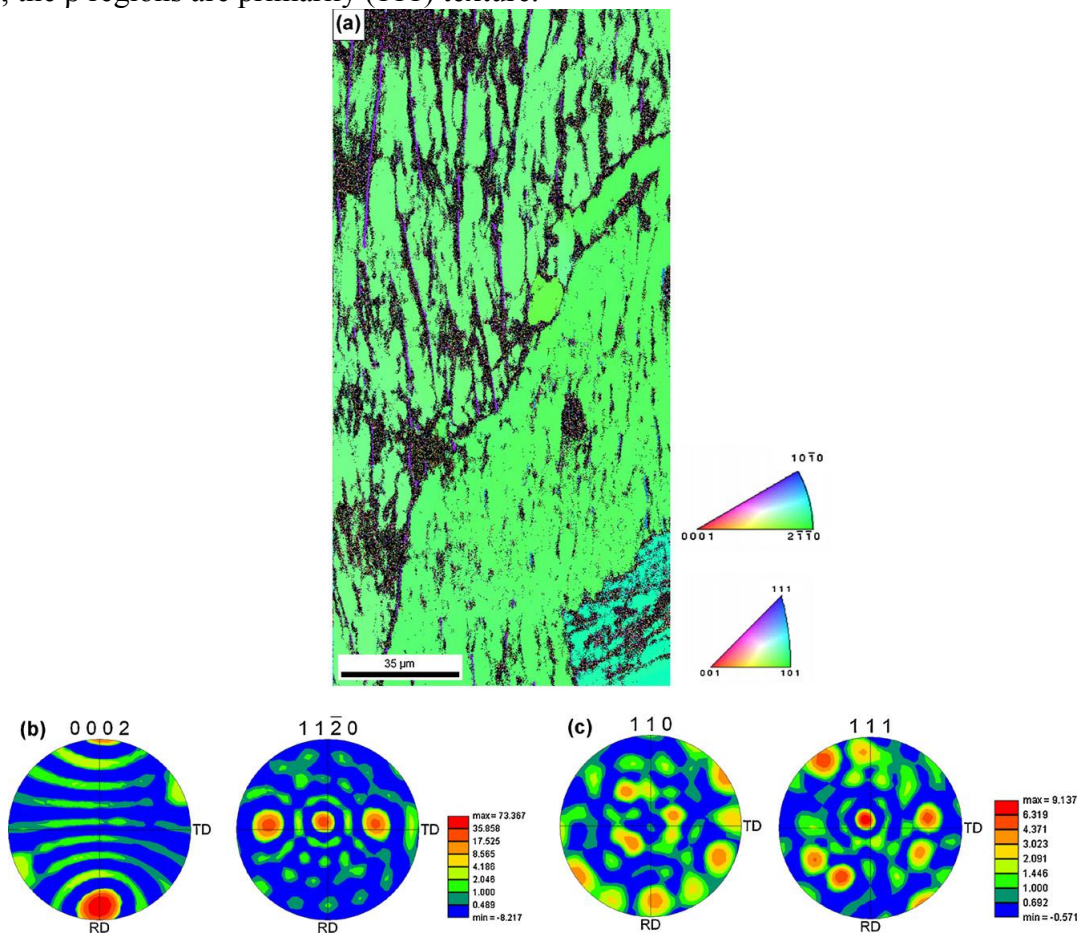

Figure 3: EBSD analysis of homogenized and slow cooled (SC) sample showing (a) crystal orientation map for the α and β -Ti phases, (b) (0002) and (11−2 0) pole figure for β-Ti.

Also contained in this figure are the pole figures for α (b) and β (c). It can be inferred that the (11-20)[0002]$_\alpha$ texture is predominant in the alpha region, while the {111}<110> type was

particularly strong in the β phase. The same procedure was also carried out for a different cooling rate, and those figure were included in my presentation. In summary, it is easy to see how useful EBSD can be for rapid identification of phase textures, and can be very useful for targeting small regions that may be difficult to identify otherwise.

Ceramics: Processing Methods for Texture Control

Ceramics have an enormous variety of modern day applications, from piezoelectrics (such as $Bi_4Ti_3O_{12}$), capacitors, insulators, superconductors, structural applications (hexagonal Boron Nitride) and use in fuel cells. While the scope of this project was initially to study the effects of phase transformations on texture, I would like to take this section to discuss the applications of texture in ceramic materials, as well as the processes that are often used.

A variety of techniques exist for processing ceramics, and while some like hot press sintering can have some control of texturing, more advanced control can be attained by use of modern procedures. Here I will illustrate one such procedure, known as Templated Grain Growth (TGG). The process is summarized fairly well in the paper produced by Jeffery A. Horn, S.C. Zhang, U. Selvaraj, Gary L. Messing, and Suzan Trolier-McKinstry titled "Templated Grain Growth of Textured Bismuth Titanate". In the introduction of this paper, Horn et al. provide the following succinct description of the TGG process.

> In this process, the orientation of the textured ceramic is determined by aligning a small percentage of anisometric grains in a matrix of fine grains. A mixture of the larger "template" particles and fine powder is oriented by a shear process (e.g., tape casting or extrusion) and sintered to produce a dense ceramic. Subsequent grain growth increases the orientation of the ceramic by the preferential growth of the template particles to yield a highly textured ceramic. [Horn et al.]

In the paper, Horn et al. apply this technique to the $Bi_4Ti_3O_{12}$ (BiT), a ferroelectric ceramic that has potential for use as a high temperature piezoelectric with a high Curie temperature (675°C). However, BiT has very low crystal symmetry (monoclinic), making it very difficult to align the polarization axes between particles. This difficulty makes BiT a perfect candidate for TGG processing, because as evidenced in Figure 3 (caption from paper), without TGG, there is very little order in the microstructure.

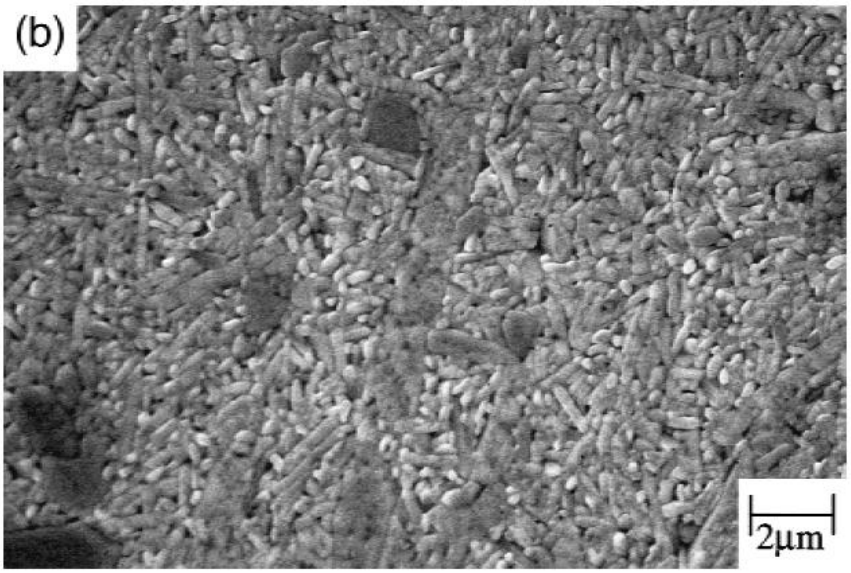

Figure 4: Edgeview of laminates containing no template particles after sintering at 1000°C for 1 hour.

In the TGG process, BiT particles (Figure 4, caption from paper) are combined with BiT platelets (Figure 5, caption from paper) into a slurry mix of powder (15%), and platelets approximately 5-10% of the powder volume. This mix was then processed by tape casting and then sintered.

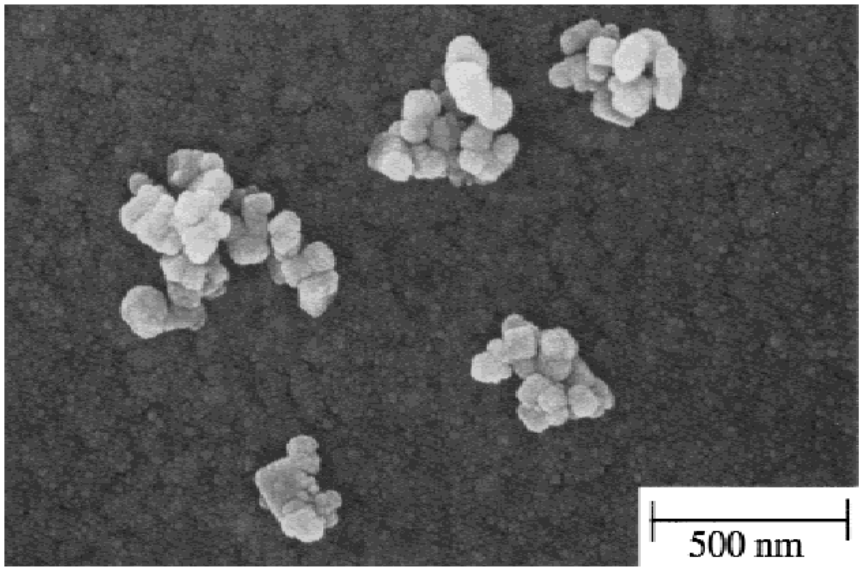

Figure 5: BiT particles calcinated at 700°C

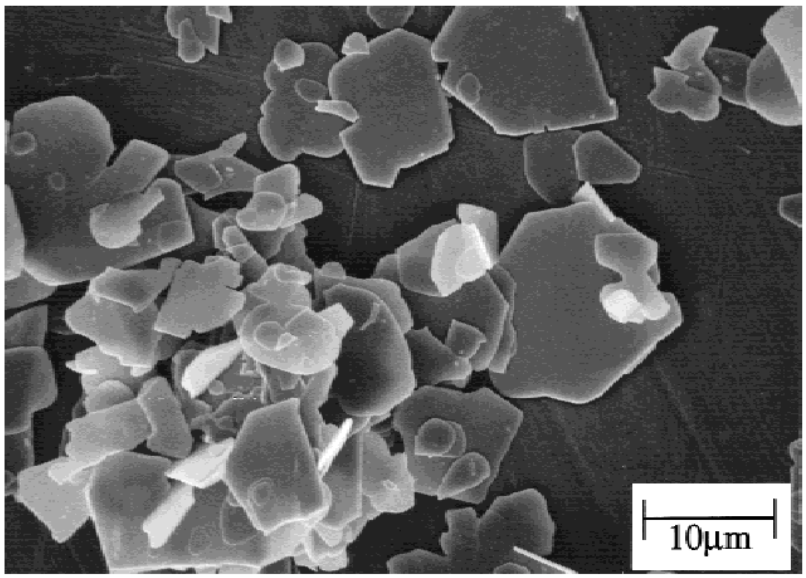

Figure 6: Molten-salt-synthesized BiT platelets.

The resulting final sintered product is illustrated in Figure 6, and as we can see it has significantly greater order in the microstructure.

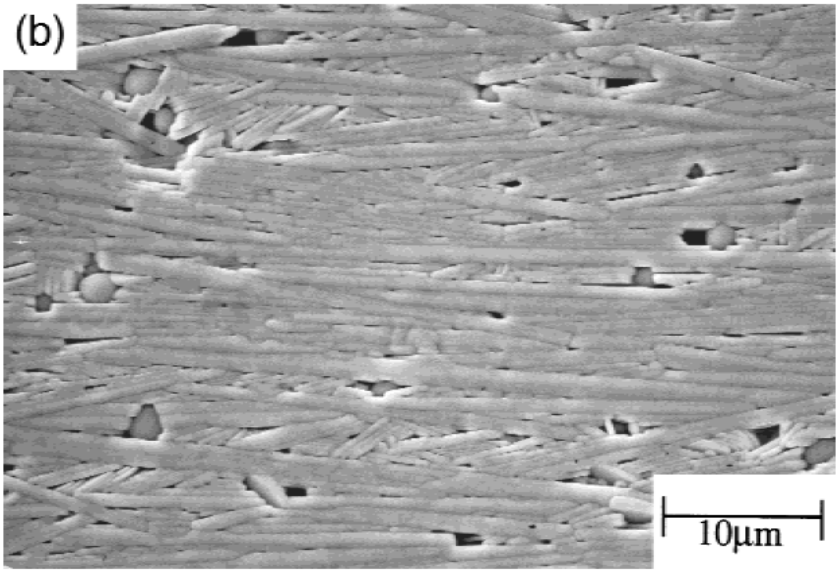

Figure 7: Edgeview of laminates containing 5 vol% platelets after sintering at 1000°C for 1 h.

In the paper, the preferred way of quantifying the degree of orientation of the particles is the degree of orientation, f, sometimes called the Lotgering factor.

$$f = \frac{p - p_0}{1 - p_0}$$

pretty simple, eh?!

$$p = \frac{\sum I_{\{00l\}}}{\sum I_{\{hkl\}}}$$

Without TGG, the laminates had an f of no higher than 0.25 regardless of sintering temperature. With TGG, f values approached 0.96 while still maintaining dense packing of the ceramic particles.

Shape Memory Alloys: Control of Texture and Properties

Shape memory alloys are a fascinating application for the problem of texture control in materials. While the kinetics and processes controlling shape memory alloys are fascinating, I would like to take some time to explore a particularly interesting method I came across in my literature search. This method is the use of neutron diffraction for monitoring the evolution of preferential textures during the deformation of shape memory alloys. The paper is "Neutron diffraction studies and multivariant simulations of shape memory alloys: Empirical texture development – mechanical response relations of martensitic nickel-titanium", put forth by Aaron Stebner, Xiujie Gao, Donald W. Brown, and L. Catherine Brinson.

Stebner et al. carried out an investigation of a common nickel-titanium shape memory alloy (NiTi, Nitinol) using the SMARTS instrument. A short summary of the instrument and sample is quoted below from the paper.

> [Fig. 8] shows a schematic of the specimen and the diffraction configuration with the diffraction plane in the plane of the paper (in-plane or top view). SMARTS accepts a pulsed white beam of neutrons generated through spallation reactions in a tungsten target and moderated by a water moderator at 283 K. The incident neutron beam impinges on a specimen and is scattered in all directions. Two detector banks consisting of 196 He-filled tubes are located 1.5 m from the specimen situated at ±90" relative to the incident beam and subtend roughly 20" in the horizontal and vertical planes. However, because the development of the texture of the specimen during deformation was of critical interest to this study, only tubes within ±5" (both horizontal and vertical) of the ±90" direction were utilized. [Stebner et al.]

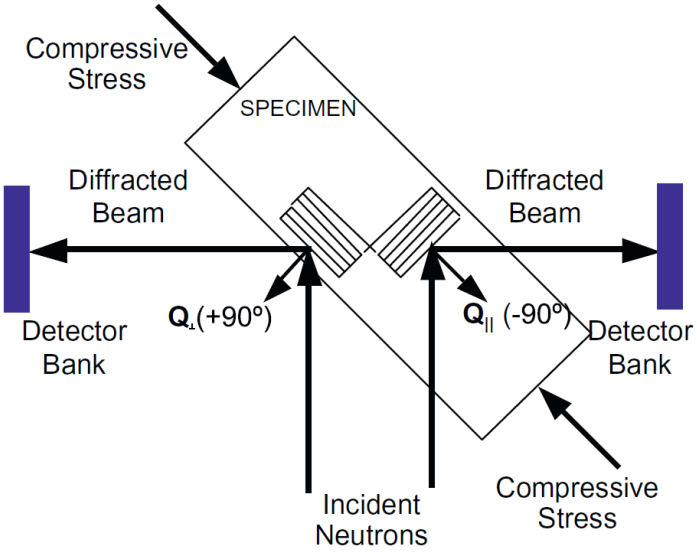

Figure 8: Schematic of the specimin and the diffraction configuration of SMARTS at LANSCE (in-plane or top view).

This technique allows researchers to track the intensity of targeted orientations as a function of time. However, this technique cannot follow all orientations, nor can it monitor them spatially. In this particular shape memory alloy, researchers were particularly interested in following the intensities of the (100) and (011) diffraction peaks, the results of which are plotted below in Figure 9, caption quoted from text.

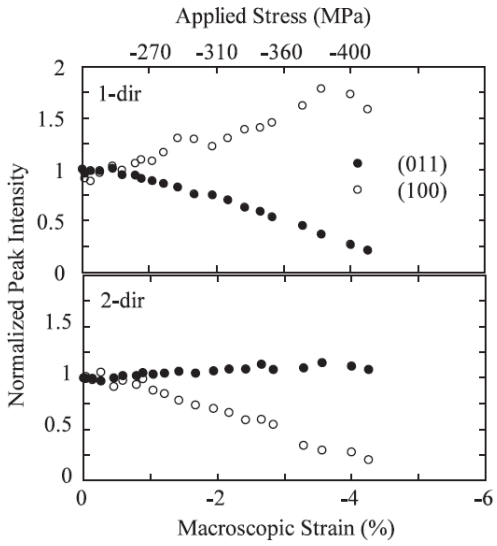

Figure 9: Normalized peak intensity as =-4.2% is applied to ϵ_{max}^{11} Specimen 1 via 1-direction compression.

Experiments were also performed comparing virgin, 3.0%, and 4.3% pre-strained samples, and the concentration of the pole intensities are compared across samples to gain a deeper understanding of shape memory alloy properties as controlled by texture. I highly recommend reviewing the paper for further details.

Composite Materials: Modern Applications and Techniques

Composites, whether examined on the micro or macro scale, are highly anisotropic. This includes whiskers, fibers, and platelets on the micro level, and composite structures such as the carbon fiber reinforced polymer laminates found on aircraft such as the Boeing 787 and various other automobiles and applications. Similarly to the ceramics section, I would like to take this opportunity to very briefly explore a processing mechanism that is particularly relevant to texture control in composite structures. The method is called Composite Reaction Texturing (CRT), and the paper reviewed for this technique is titled "Composite reaction texturing of superconducting ceramic composites", written by B. Soylu, N. Adamopoulos, D.M. Glowacka, and J.E. Evetts. In their paper, they aim to address the problem with low critical current densities in the high temperature superconductor $Bi2Sr2Ca_1Cu2O8_{+a}$. They describe the CRT process as follows.

> (CRT)[7], which is a texturing process performed by seeding the superconducting phase with a dense aligned distribution of inert second-phase particles of a suitable geometry (e.g., MgO whiskers) and reacting the composite to nucleate and grow the superconducting phase with a texture determined by this second phase. [Soylu et al.]

In other words, they are able to lay out a template of the intended microstructure, and upon combination and reaction with their intended phase they are able to construct this microstructure to attain the desired texture. The process can be simplified in the figure below, caption quoted directly from paper.

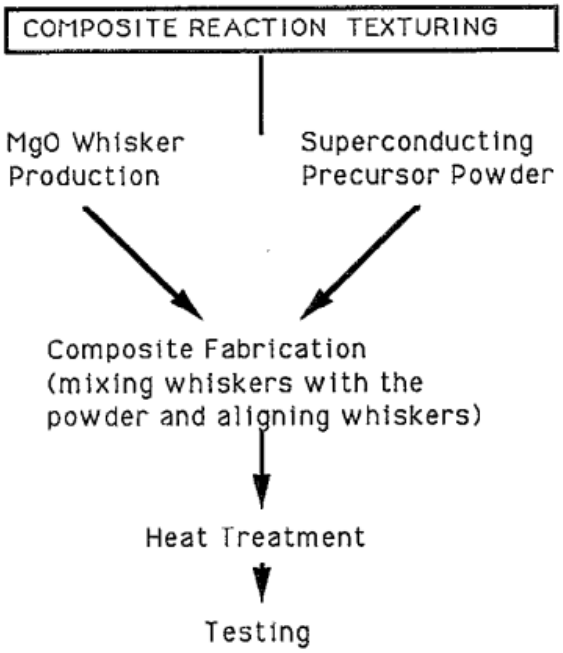

Figure 10: Flowchart of the composite reaction texturing method.

Differences in the uniformity of the MgO fibers can result in small differences in texture through the sample, but the ultimate result is a highly aligned sample, as evidenced in the following figure (caption from text).

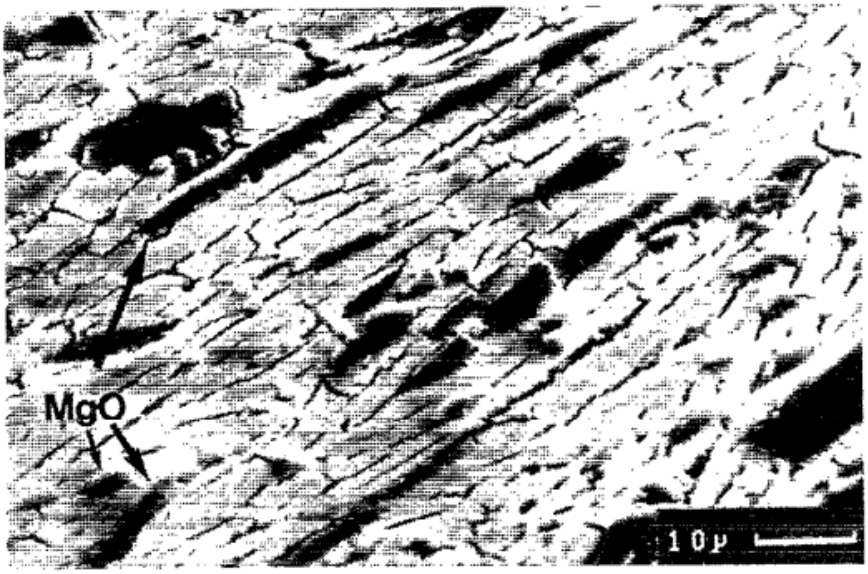

Figure 11: SEM micrograph showing a well-aligned cross-sectional area from a specimen which was etched to reveal the grain boundaries of long aligned 2212 plates. The raised particles (arrowed) are sections of MgO whiskers with random planar distribution.

Ultimately, this degree of control over the microstructure resulted in an improvement in the transport critical-current density J_{ct} from less than 500 A cm^{-2} at 77K in the specimen not seeded with MgO, to 4500 A cm^{-2} at 77K in the sample seeded with MgO.

Concluding Remarks

It is clearly apparent that every class of materials has relevant applications for texture control and analysis, and significant research is being done in these fields. I have tried to provide a summary of the modern tools, techniques, and knowledge in each area, but I feel that I have only scratched the surface in this paper. There are numerous papers and topics available for exploration, each of which gives rise to a brand new series of questions for exploration.

Since I forgot to mention during my presentation what I took out of the class I will put it here.

Traditionally I've been more geared towards the engineering side of materials science & engineering, particularly interested in the applications, and through this class I was introduced to a very useful new tool for materials analysis, one that I may not otherwise have been aware of. While we were introduced to slip systems and microstructure as undergraduates, I had no idea the degree to which the orientations of the grains inside the crystal had an effect on the properties of the material at hand. affect

References

Chen, M., Glowacka, D., Soylu, B., Watson, D., Christiansen, J., Baranowski, R., Evetts, J. (1995, June). Texture and Critical Current Anisotropy in Composite Reaction Textured MgO Whisker/Bi-2212 Multilayer Structures. *IEEE Transactions on Applied Superconductivity, 5*(2), 1467-1470.

Horn, J. A., Zhang, S. C., Selvaraj, U., Messing, G. L., & Trolier-McKinstry, S. (1999). Templated Grain Growth of Textured Bismuth Titanate. *Am. Ceram. Soc., 82*(4), 921-926.

T. Karthikeyan, Arup Dasgupta, R. Khatirkar, S. Saroja, I. Samajdar, M. Vijayalakshmi, Effect of cooling rate on transformation texture and variant selection during β → α transformation in Ti–5Ta–1.8Nb alloy, Materials Science and Engineering: A, Volume 528, Issue 2, 15 December 2010, Pages 549-558, ISSN 0921-5093, 10.1016/j.msea.2010.09.055. (http://www.sciencedirect.com/science/article/pii/S0921509310010853)

Kenfaui, D., Chateigner, D., Gomina, M. and Noudem, J. G. (2011), Anisotropy of the Mechanical and Thermoelectric Properties of Hot-Pressed Single-Layer and Multilayer Thick $Ca_3Co_4O_9$ Ceramics. International Journal of Applied Ceramic Technology, 8: 214–226. doi: 10.1111/j.1744-7402.2009.02431.x

H.Y. Kim, T. Sasaki, K. Okutsu, J.I. Kim, T. Inamura, H. Hosoda, S. Miyazaki, Texture and shape memory behavior of Ti–22Nb–6Ta alloy, Acta Materialia, Volume 54, Issue 2, January 2006, Pages 423-433, ISSN 1359-6454, 10.1016/j.actamat.2005.09.014. (http://www.sciencedirect.com/science/article/pii/S1359645405005392)

D.A Molodov, A.D Sheikh-Ali, Effect of magnetic field on texture evolution in titanium, Acta Materialia, Volume 52, Issue 14, 16 August 2004, Pages 4377-4383, ISSN 1359-6454, 10.1016/j.actamat.2004.06.004. (http://www.sciencedirect.com/science/article/pii/S1359645404003349)

Ray, R. K., Jonas, J. J., Hook, R. E., Institute of Materials (London, England), & ASM International. (1994). *Cold rolling and annealing textures in low carbon and extra low carbon steels*. London: Institute of Materials.

Aaron Stebner, Xiujie Gao, Donald W. Brown, L. Catherine Brinson, Neutron diffraction studies and multivariant simulations of shape memory alloys: Empirical texture development–mechanical response relations of martensitic nickel–titanium, Acta Materialia, Volume 59, Issue 7, April 2011, Pages 2841-2849, ISSN 1359-6454, 10.1016/j.actamat.2011.01.023. (http://www.sciencedirect.com/science/article/pii/S1359645411000292)

Soylu, B.; Adamopoulos, N.; Glowacka, D. M.; Evetts, J. E.; , "Composite reaction texturing of superconducting ceramic composites," *Applied Physics Letters*, vol.60, no.25, pp.3183-3185, Jun 1992 (http://ieeexplore.ieee.org/stamp/stamp.jsp?tp=&arnumber=4878550&isnumber=4878514)